

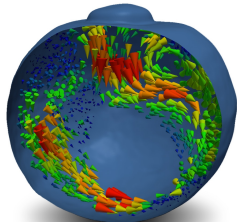
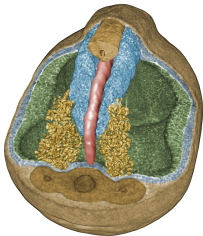
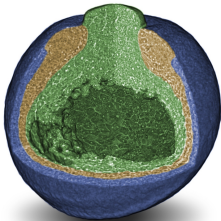


X-ray phase-contrast in vivo tomography

Julian Moosmann

KTH Royal Institute of Technology, Stockholm

SFB 755 Seminar, November 5th, 2015, Göttingen



Outline

Propagation-based X-ray phase-contrast

- Introduction to phase-contrast

- Experimental setup

- Phase retrieval

In vivo X-ray phase-contrast tomography

- Motivation

- Comparison with other techniques

- Considerations for in vivo imaging

- Application

Outline

Propagation-based X-ray phase-contrast

- Introduction to phase-contrast

- Experimental setup

- Phase retrieval

In vivo X-ray phase-contrast tomography

- Motivation

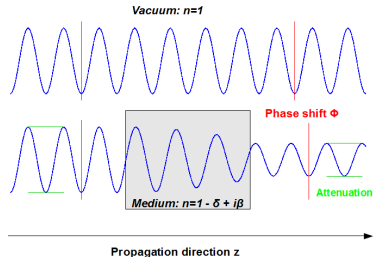
- Comparison with other techniques

- Considerations for in vivo imaging

- Application

Introduction

- ▶ Hard X-rays are strongly penetrating electromagnetic waves
- ▶ Interaction of X-ray and matter described by refractive index



$$n = 1 - \delta + i\beta$$

- ▶ Transmitted wave front: $\Psi_0 = \sqrt{I_0} \exp(i\phi_0)$
- ▶ Absorption: destructive

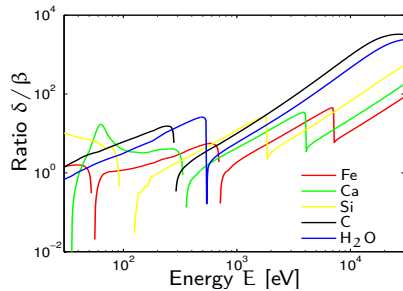
$$\sqrt{I_0} = \sqrt{I_{in}} \frac{2\pi}{\lambda} \int dz \beta(z)$$

- ▶ Phase: sensitive to soft-tissues

$$\phi_0 = \frac{2\pi}{\lambda} \int dz \delta(z)$$

Introduction

- ▶ Energy-dependence of refractive index



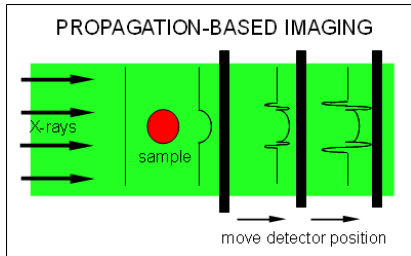
- ▶ Use monochromatic coherent X-ray with energies s.t.

$$\frac{\delta}{\beta} \gg 1$$

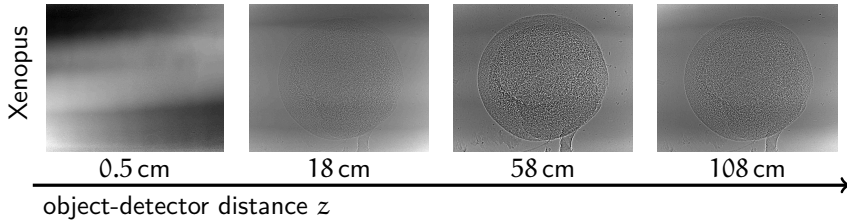
- ▶ Phase-contrast imaging of weakly absorbing materials

Propagation-based phase contrast

- ▶ Simple setup: no additional optics, no scanning, no stepping
 - ▶ stable, fast, efficient
- ▶ Intensity contrast emerges via free-space propagation of transmitted wave field



Sequence of intensity maps I_z : signal increases with z



Outline

Propagation-based X-ray phase-contrast

- Introduction to phase-contrast

- Experimental setup

- Phase retrieval

In vivo X-ray phase-contrast tomography

- Motivation

- Comparison with other techniques

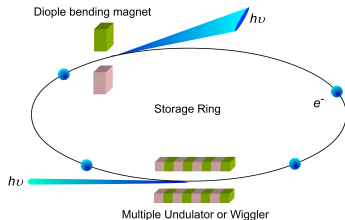
- Considerations for in vivo imaging

- Application

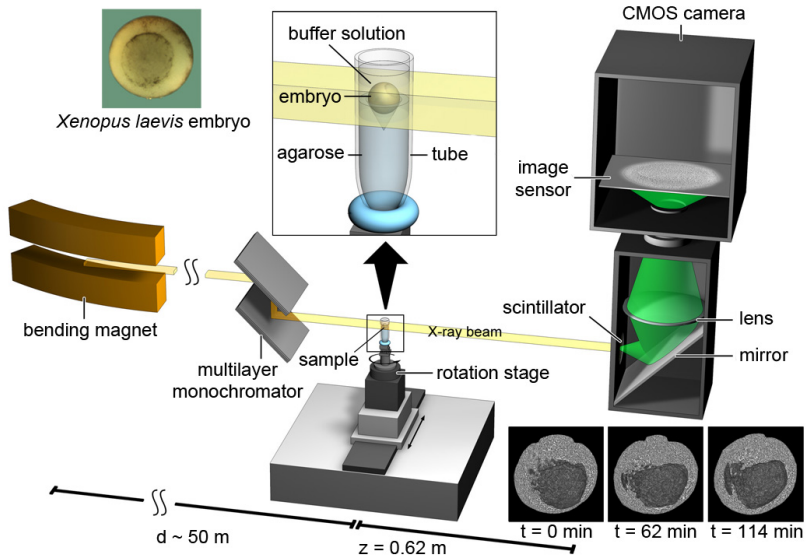
X-ray source

Synchrotron radiation is required

- ▶ High flux
 - ▶ High spatial resolution
 - ▶ Fast acquisition: image fast cell movement, high throughput
- ▶ Coherence
 - ▶ propagation-base phase-contrast
- ▶ Quasimonochromatic spectrum (single harmonic or monochromator)
 - ▶ Reduce dose
 - ▶ Propagation-base phase-contrast



Experimental setup



Outline

Propagation-based X-ray phase-contrast

Introduction to phase-contrast

Experimental setup

Phase retrieval

In vivo X-ray phase-contrast tomography

Motivation

Comparison with other techniques

Considerations for in vivo imaging

Application

Phase contrast

- ▶ Rewrite Fresnel diffraction integral

$$\mathcal{F}I_z(\xi) = \int d\mathbf{x} \exp(-i2\pi\mathbf{x} \cdot \xi) \Psi_0(\mathbf{x} - \frac{\lambda z}{2}\xi) \Psi_0^*(\mathbf{x} + \frac{\lambda z}{2}\xi)$$

\mathcal{F} : Fourier transform, $\mathbf{x}, \xi \in \mathbb{R}^2$ [Guigay 1977]

- ▶ Intensity contrast $g_z = I_z/I_0 - 1$
- ▶ Expand exponential of exit wave field $\Psi_0 = \sqrt{I_0} \exp(i\phi_0)$
- ▶ Guigay up to $\mathcal{O}(\phi_0)$ (pure-phase object)

$$\begin{aligned} \mathcal{F}g_z(\xi) &= 2 \sin(\pi\lambda z \xi^2) \mathcal{F}\phi_0(\xi) \\ &\quad - \cos(\pi\lambda z \xi^2) \int d\xi' \mathcal{F}\phi_0(\xi') \mathcal{F}\phi_0(\xi - \xi') \\ &\quad + \exp(i\pi\lambda z \xi^2) \int d\xi' \exp(-i2\pi\lambda z \xi \cdot \xi') \mathcal{F}\phi_0(\xi') \mathcal{F}\phi_0(\xi - \xi') \end{aligned}$$

Phase contrast

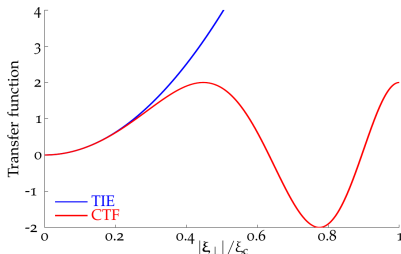
Linear approximations

- ▶ Contrast transfer function (CTF)
 - ▶ Weakly varying phase: $|\phi_0(x + \frac{\lambda z}{2} \xi) - \phi_0(x - \frac{\lambda z}{2} \xi)| \ll 1$

$$\mathcal{F}g_z(\xi) = 2 \sin(\pi \lambda z \xi^2) \mathcal{F}\phi_0(\xi)$$

- ▶ Linearised transport-of-intensity equation (TIE)
 - ▶ Edge-enhancement regime: small propagation distance

$$\mathcal{F}g_z(\xi) = 2\pi \lambda z \xi^2 \mathcal{F}\phi_0(\xi)$$



Phase retrieval

Linear models

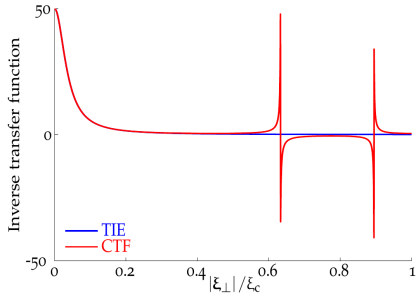
- ▶ Contrast transfer function (CTF)
 - ▶ High resolution
 - ▶ Limited to weakly varying phases

$$\mathcal{F}\phi_0(\xi) = \frac{\mathcal{F}g_z(\xi)}{2 \sin(\pi\lambda z \xi^2)}$$

[Guigay 1977; Gureyev et al. 2006; Cloetens 1998]

- ▶ Linearised TIE: Paganin phase retrieval
 - ▶ Valid for small propagation distance
 - ▶ Low-pass filter for large z

$$\mathcal{F}\phi_0(\xi) = \frac{\mathcal{F}g_z(\xi)}{2\pi\lambda z \xi^2}$$



Phase retrieval

Problem

- ▶ Weak intensity contrast g_z at small z
 - ▶ Noise-to-signal in $I_z \propto \frac{1}{\sqrt{z}}$
 - ▶ Noise in $\phi_0 \propto \frac{1}{z}$
 - Measure at large z
- ▶ At large z : low resolution for Paganin phase retrieval
 - CTF phase retrieval
- ▶ Extended objects (eg Xenopus embryos) exhibit phase variations of order $\mathcal{O}(1 \text{ rad})$
- ▶ CTF phase retrieval fails (quasiperiodic artifacts)

What to do? → Phase retrieval beyond linear approximations

Nonlinear phase retrieval

TIE beyond linearity

- ▶ Systematic expansion of g_z and ϕ_z in powers of z
- ▶ Expansion coefficients determined full paraxial wave equation (TIE is the imaginary part of PWE)
- ▶ Nonlinear corrections to ϕ_0 :

$$\nabla_{\perp}^2 \phi_0 = -\frac{k}{z} g_z + \frac{z}{2k} \left[(\nabla_{\perp}^2 \phi_0)^2 + \frac{1}{2} \nabla_{\perp}^2 (\nabla_{\perp} \phi_0)^2 + (\nabla_{\perp} \nabla_{\perp}^2 \phi_0) \cdot \nabla_{\perp} \phi_0 \right]$$

- ▶ Perturbation theory: evaluate correction in terms of leading order result (Paganin)
- ▶ → Quantitative improvement of reconstructed phases
- ▶ But: low resolution due to leading order

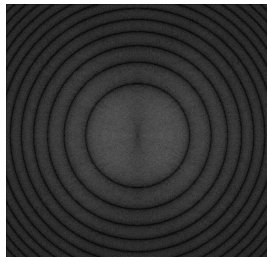
[Moosmann et al., Opt. Express 2010]

What else? → Consider contrast transfer function

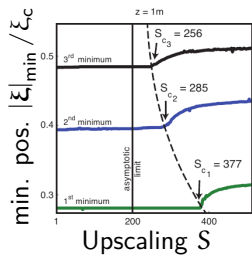
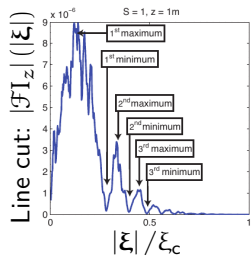
Evolution of intensity contrast

Examine contrast transfer from phase to intensity

- ▶ Compute intensity contrast from input phase map (Lena)
- ▶ Amplify phase variations by upscaling of input phase
- ▶ Consider Fourier transformed intensity as a function of phase upscaling



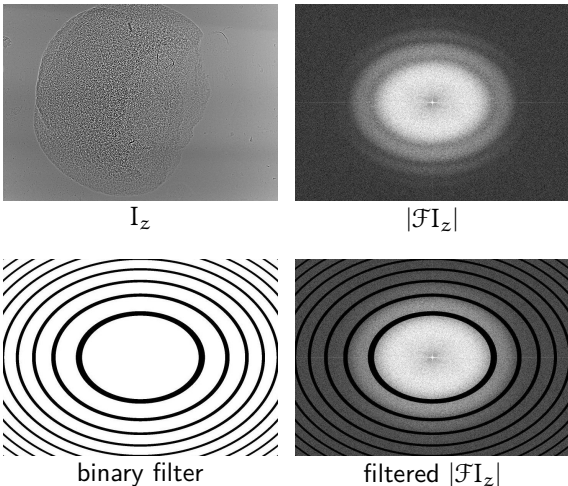
$|\mathcal{F}I_z|(\xi)$



Phase retrieval: quasiparticle approach

- ▶ Fourier space filter: crop regions around minima
- ▶ Phase retrieval via CTF using filtered intensity

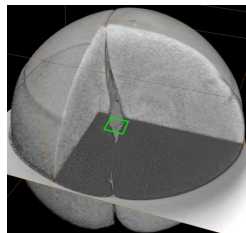
Data: TopoTomo@ANKA



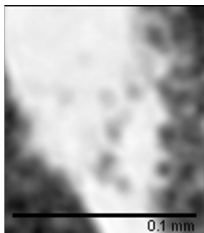
[Moosmann et al., Opt. Express 2011]

Tomography: Paganin vs CTF vs QP

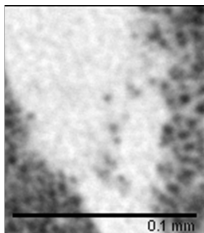
Xenopus, fixed, 4-cell stage, ID19@ESRF, $E = 20 \text{ keV}$,
 $\Delta E/E = 10^{-4}$, $z = 1 \text{ m}$, $\Delta x = 0.75 \mu\text{m}$, 1600 projections



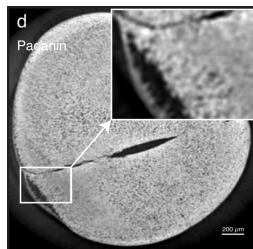
Rendering



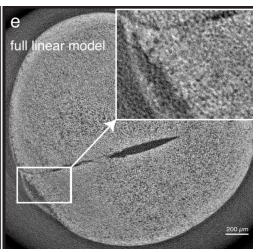
Paganin



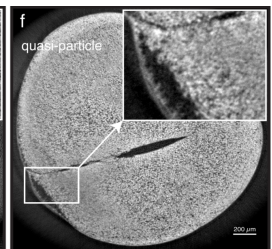
Quasiparticle



Paganin



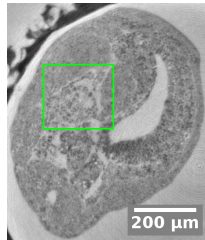
CTF



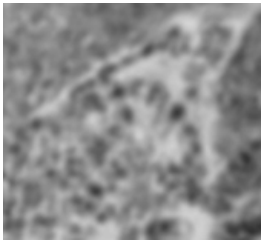
Quasiparticle

In vivo tomography: Paganin vs QP

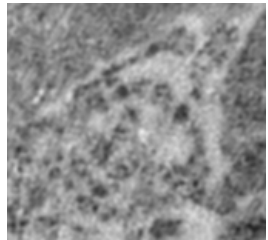
Xenopus, in vivo, stage 23, ID19@ESRF, $E = 26.2 \text{ keV}$,
 $\Delta E/E \approx 0.15$ (single harmonic), $z = 3.6 \text{ m}$, $\Delta x = 1.6 \mu\text{m}$, 500
projections



tomogram slice



Paganin, zoom



quasiparticle, zoom

Outline

Propagation-based X-ray phase-contrast

- Introduction to phase-contrast

- Experimental setup

- Phase retrieval

In vivo X-ray phase-contrast tomography

- Motivation

- Comparison with other techniques

- Considerations for in vivo imaging

- Application

Motivation: in vivo imaging

- ▶ Applications in Life Sciences: Imaging techniques to study the development of model organisms are essential tools in Developmental Biology, Medicine, Toxicology, Zoology, . . .
- ▶ Aim: Visualisation of developmental processes
 - ▶ Division, differentiation, shape changes, & trajectories of single cells
 - ▶ Identify (new) morphological structures
 - ▶ Movement & separation of tissues
 - ▶ Cavity formation
 - ▶ Propulsion mechanism
- ▶ Biological specimen w/o cartilage, bone, & blood vessels are essentially pure-phase objects for $E > 20 \text{ keV}$
- ▶ Examples of important vertebrate model organisms



Xenopus laevis



zebrafish



lamprey

Outline

Propagation-based X-ray phase-contrast

- Introduction to phase-contrast

- Experimental setup

- Phase retrieval

In vivo X-ray phase-contrast tomography

- Motivation

- Comparison with other techniques**

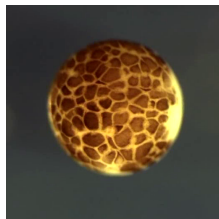
- Considerations for in vivo imaging

- Application

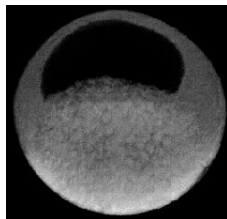
Comparison of in vivo imaging techniques

Optical light microscopy

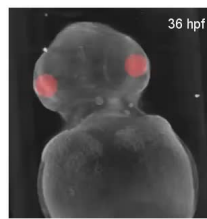
- ▶ non-destructive
- ▶ restricted to surfaces or transparent samples
- ▶ destructive: sectioning of fixed embryos
- ▶ spatial resolution $\sim 1 \mu\text{m}$



Xenopus: surface



Xenopus: surface,
sectioned



Zebrafish: optical
projection tomography

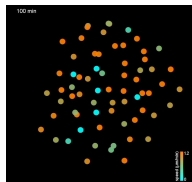
[Williams & Smith; Danilchik; Bassi et al.]

Comparison of *in vivo* imaging techniques

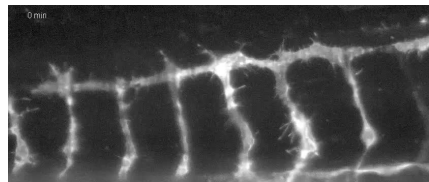
Fluorescence microscopy

- ▶ non-destructive
- ▶ transparent objects
- ▶ depth information limited to few cell layers
- ▶ Labelling: expression of fluorescence marker required
- ▶ photobleaching
- ▶ sparse spatial information
- ▶ spatial resolution $\sim 1 \mu\text{m}$

Zebrafish



light-sheet microscopy

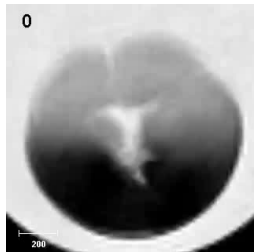


selective plane illumination microscopy

Comparison of in vivo imaging techniques

Magnetic Resonance Imaging

- ▶ non-destructive
- ▶ dense & deep spatial information
- ▶ spatial resolution $\sim 25 \mu\text{m}$
- ▶ temporal resolution
 $\sim 1 \text{ h/tomogram}$



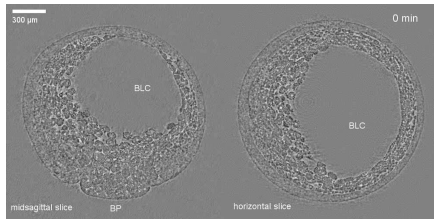
Xenopus: MRI

[Papan et al.]

Comparison of in vivo imaging techniques

X-ray phase-contrast microtomography (PC μ CT)

- ▶ apt for optically opaque objects
- ▶ fast
- ▶ dense spatial information
- ▶ destructive: possible time lapse $\lesssim 2$ h
- ▶ spatial resolution $\sim 1 \mu\text{m}$



Xenopus: X-ray PC μ CT

[Moosmann et al., Nature; Moosmann et al., Nature Protocols]

Digital study

Using dense & deep 3D information allows to digitally study

- ▶ Structural changes, gene expression, perturbation experiments (signal transduction, functioning of gene regulatory networks, ...)
- ▶ Cell and tissue dynamics: exchange of fluids and nutrients, transient structures, cell migratory behaviour, ...
- ▶ Propulsion mechanisms for cell and tissue migration: differential flow-field analysis (convergent extension, cell-cell adhesion, cell-matrix interaction, ...)

Outline

Propagation-based X-ray phase-contrast

- Introduction to phase-contrast

- Experimental setup

- Phase retrieval

In vivo X-ray phase-contrast tomography

- Motivation

- Comparison with other techniques

- Considerations for in vivo imaging

- Application

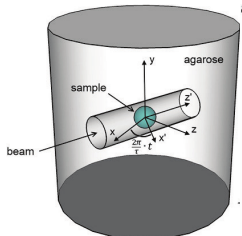
Considerations for in vivo imaging

- ▶ Motion blurring due to cell movement: $\sim 4 \mu\text{m}/\text{min}$
 - ▶ Acquisition time for tomogram at resolution: $\lesssim 30 \text{ s}$
 - ▶ Required flux density: $> 10^{12} \text{ photons/s/mm}^2$
- ▶ Dose effects: heat load, double-strand breaking, radiolysis of water \rightarrow free radicals
- ▶ Setup: parameter optimisation
 - ▶ Energy: dose vs photon flux vs phase contrast vs detection efficiency
 - ▶ Exposure time: dose vs signal-to-noise vs motion blurring
 - ▶ Object-detector distance: signal-to-noise vs blurring (finite source size, coherence, nonlinear propagation effects)
 - ▶ Tomography: number of projection, dose, resolution, rotation blurring, ...

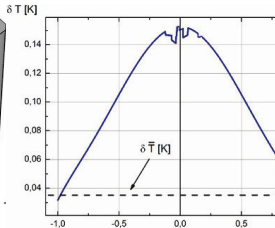
Dose effect: heat load

Compare simulation and measurement of temperature profile

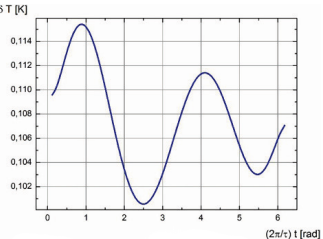
- ▶ Simulation of temperature profile: solve heat equation numerically, energy: 30 keV, flux: 10^{12} photons/s/mm/square



schematic of
sample environment



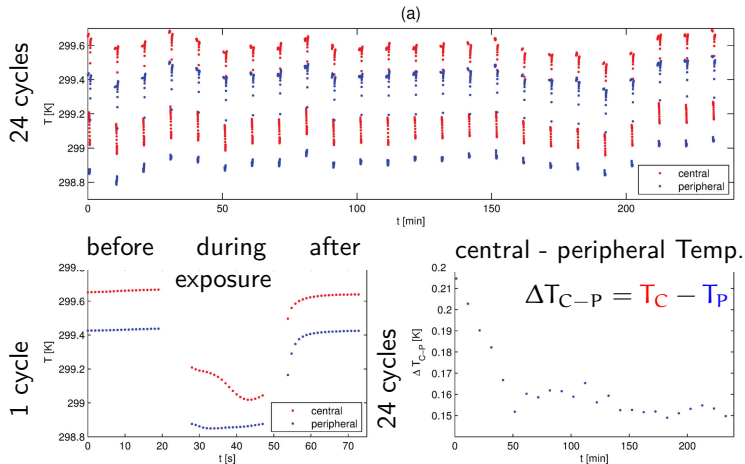
radial
temperature profile



angular
temperature profile

Dose effect: heat load

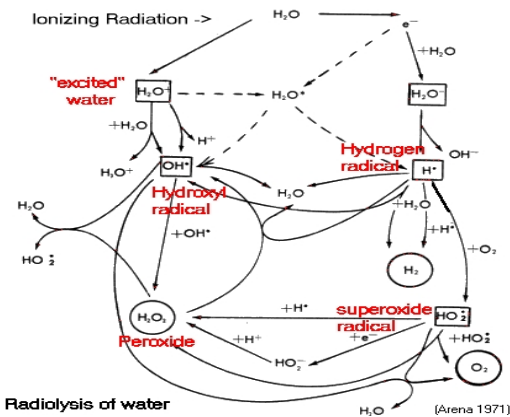
- ▶ Measurement of temperature: setup identical to in vivo experiment



Dose effect: radiolysis of water

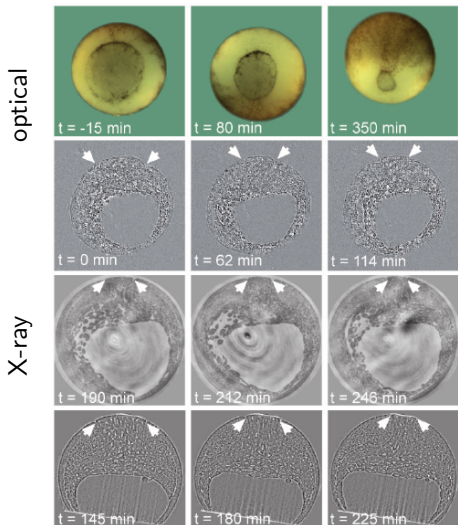
Ionising radiation induces radiolysis of water molecules

- Radicals (H_3O^+ , $\text{HO}\cdot$, e_{aq}^- , $\text{H}\cdot$) and highly reactive oxygen species (HO_2 , H_2O_2 , ...) inflict oxidative damage to cell molecules and DNA

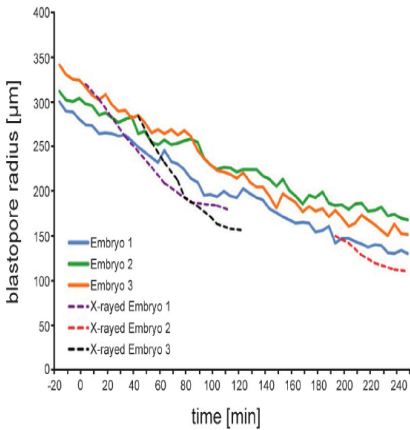


Viability

Compare key morphogenetic processes in X-rayed & optical-light viewed embryos. Eg consider blastopore closure

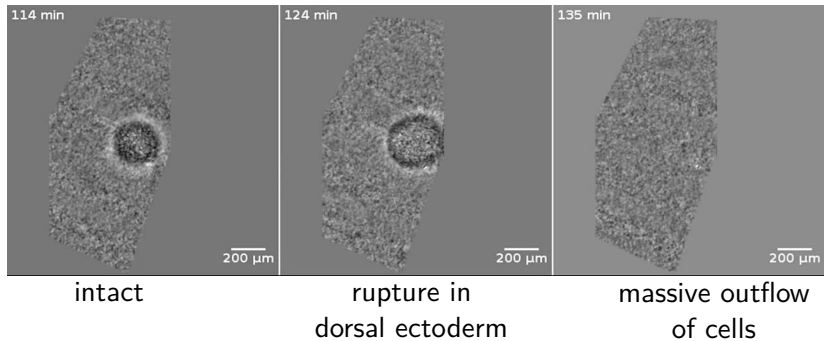


► Rate of blastopore closure



Radiolysis-induced degradation of embryo

- ▶ Sagittal slicing through tomograms at 114 min, 124 min, 135 min after first X-ray scan

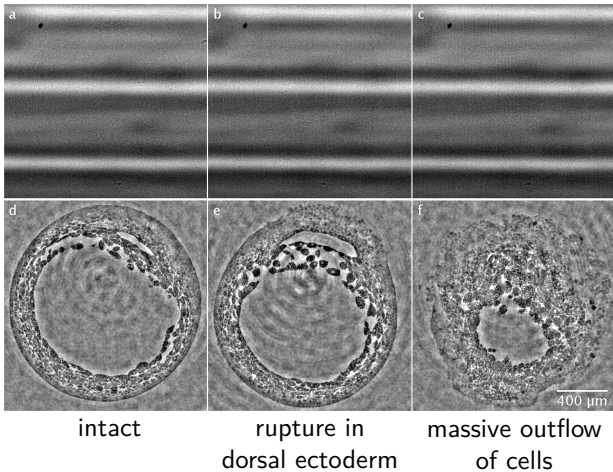


optical
image



Degradation of embryo

Raw projections and corresponding slice through tomograms



- ▶ Need for fast/online reconstructions to decide when to terminate scan

Outline

Propagation-based X-ray phase-contrast

- Introduction to phase-contrast

- Experimental setup

- Phase retrieval

In vivo X-ray phase-contrast tomography

- Motivation

- Comparison with other techniques

- Considerations for in vivo imaging

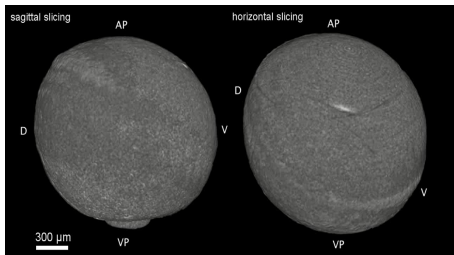
- Application

4D *in vivo* tomography

Xenopus gastrulation:

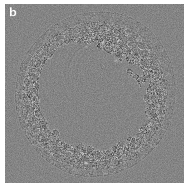
2-BM@APS, time lapse: 2 h,
time between tomograms:

10 min, $\Delta x=1\text{ }\mu\text{m}$, $E=30\text{ keV}$,
 $\Delta E/E=10^{-2}$

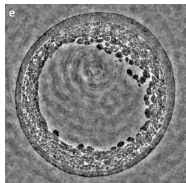


Slicing through rendered volume

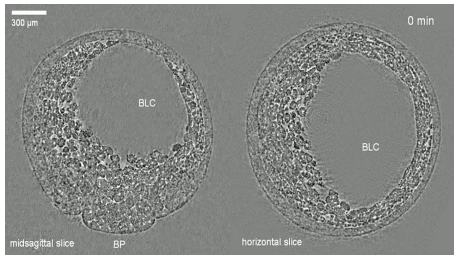
tomographic reconstruction



intensity



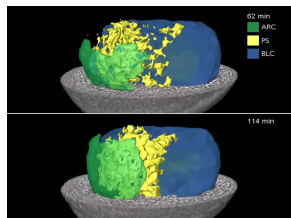
phase



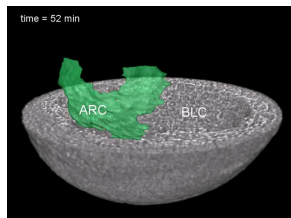
Time-lapse of reconstructed central slice

Segmentation & volume analysis

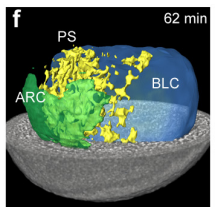
What drives the archenteron inflation?



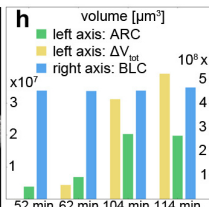
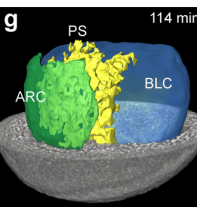
Segmented cavities



Inflating archenteron



Archenteron inflation

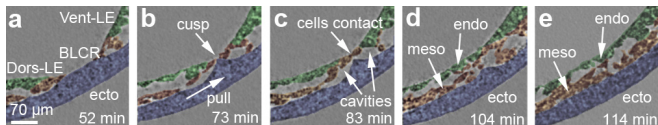


Volume balancing

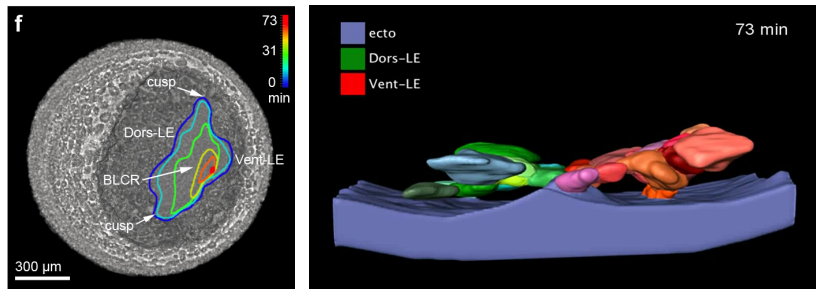
- Conclusion: inflation is driven by uptake of external water

Observation of unreported transient structure

- ▶ Confrontation of head & ventral mesendoderm: formation of a transient ridge
- ▶ Not observable in fixed embryos or explants



Time lapse of reconstructed slice



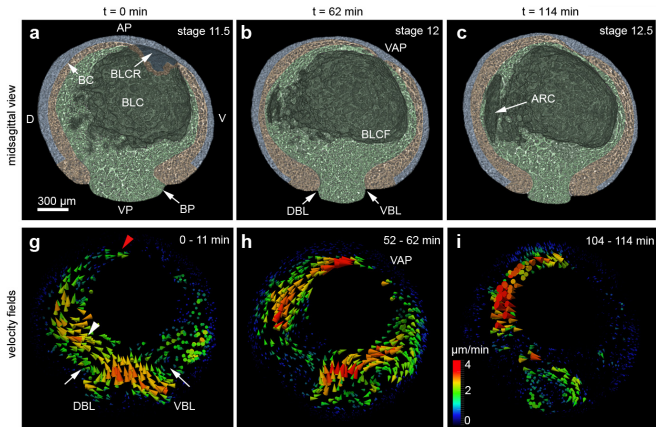
Moving contour of leading-edge mesendoderm

Segmented structures

Optical flow

Flow field ν visualises overall dynamics

Rendering of
halved embryo



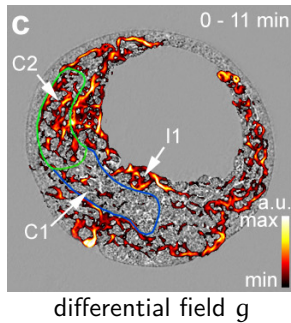
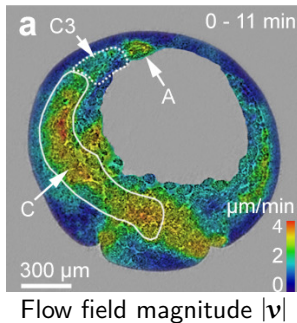
Velocity field
on central slab

- ▶ Collective cell movements within the gastrula reveals
 - ▶ rotation of vegetal endoderm (g: white arrowhead)
 - ▶ involution of mesendoderm at dorsal & ventral blastopore lip (g: white arrows)

Differential optical flow

Differential field $g = |\nabla v_x| + |\nabla v_y| + |\nabla v_z|$ visualises differential cell & tissue motion*

- ▶ Collective vs individual movement
- ▶ Propulsion mechanisms



C1: collective motion driven by blastopore closure

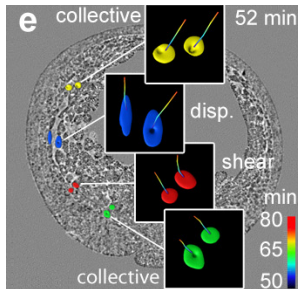
C2: collective motion driven by involution of dorsal mesendoderm plus relative cell motion driven by mediolateral intercalation associated with convergent extension

I1: crawling of individual cell on blastocoel floor

* non-isotropic definition of g (L2- instead of L1-norm) also capture directional deviations at constant $|v|$

Integrated optical flow

- ▶ Cell tracking via time integration of flow field



Trajectories of cell pairs

Summary

- ▶ Quasiparticle approach provides a high-resolution phase retrieval at large propagation distances and strongly varying phases typical for *in vivo* imaging
- ▶ Propagation-based, single-distance X-ray phase-contrast tomography in combination with optical flow analysis is a useful tool for 4D *in vivo* investigations in developmental biology

Outlook

Experiment

- ▶ 4th generation synchrotron upgrades (multi-bend achromat lattices): drastically enhanced coherence & brilliance → enhanced contrast, allows larger z
- ▶ Cone-beam magnification (Kirkpatrick Baez mirrors, ...)
- ▶ Optimisation of detector system and tomographic acquisition: scintillator, microscope, camera
- ▶ Optimisation of tomographic acquisition: stepping vs on-the-fly, fast shutter,
- ▶ Combine X-ray phase-contrast & fluorescence microscopy or optical projection tomography
- ▶ Systematic dose studies: dose delay effects, find phenomenological function describing dose expression effects,
...

Outlook

Theory & Algorithms

- ▶ Adopt quasiparticle approach for transmission electron microscopy
- ▶ Variational (iterative) methods from optimisation theory: total variation regularisation, sparsity (compressed sensing), dictionary learning, neural networks, wavelets/shearlets, ...
- ▶ Modelling of noise, blurring (scintillator, ...), point spread function (MLEM, deconvolution, etc)

Biology

- ▶ Perturbation experiments (wildtype vs morphant embryos): role of adhesion molecules, signalling pathways, transcription factors, gene regulatory networks, ...
- ▶ Recent & upcoming experiments: emigration & delamination processes of neural crest cells as a model for on-set of cancer metastasis

Acknowledgement

- ▶ Karlsruhe Institute of Technology
 - ▶ Ralf Hofmann
 - ▶ Jubin Kashef
 - ▶ Tilo Baumbach
 - ▶ Alexey Ershov
 - ▶ Venera Weinhard
 - ▶ Daniel Hänschke
- ▶ Advanced Synchrotron Source
 - ▶ Xianghui Xao
- ▶ European Synchrotron Radiation Facility
 - ▶ Lukas Helfen
 - ▶ Alexander Rack
- ▶ Northwestern University
 - ▶ Carole LaBonne
 - ▶ Maneeshi Prasad
- ▶ KTH - Royal Institute of Technology
 - ▶ Ozan Öktem

Optimal propagation distance

Spatio-temporal coherence constrains propagation distances

- ▶ Given a transversal coherence length l_t determined by the Van-Zittert Zernike theorem and satisfying

$$l_t \geq \frac{\lambda z}{2\Delta x} = \lambda z \xi_c \geq \lambda z |\xi|$$

λ : wave length, z : propagation distance, Δx : pixel size

- ▶ Given a longitudinal coherence length l_l determined by

$$l_l = \frac{ch}{\Delta E}$$

c : speed of light, h : Planck's constant, ΔE : bandwidth

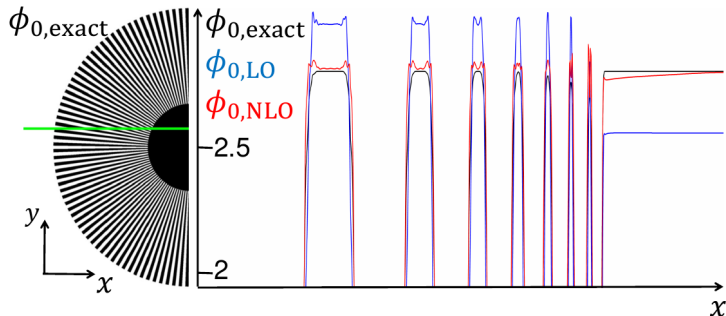
- ▶ Window of optimal propagation distances is given by

$$\frac{l_t^2}{2l_l} \leq z \leq \frac{d\Delta x}{s}$$

d : source-sample distance, s : source size

Nonlinear phase retrieval: Beyond linear TIE

Simulation: Siemens star test pattern, $E = 30\text{keV}$, $z = 0.3\text{m}$



$\phi_{0,\text{exact}}$: exact phase map

$\phi_{0,\text{LO}}$: phase map to leading order (Paganin)

$\phi_{0,\text{NLO}}$: phase map to next-to-leading order (Paganin plus nonlinear correction)